Assembly of a [2Fe-2S]$^{2+}$ Cluster in a Molecular Variant of *Clostridium pasteurianum* Rubredoxin†

Jacques Meyer,*,‡ Jean Gagnon,§ Jacques Gaillard,|| Marc Lutz,⊥ Catalina Achim,@ Eckard Münck,@ Yves Pétillot,§ Christopher M. Colangelo,# and Robert A. Scott#

Département de Biologie Moléculaire et Structurale, CEA-Grenoble, 38054 Grenoble, France, Institut de Biologie Structurale, CEA-CNRS, 38027 Grenoble, France, Département de Recherche Fondamentale sur la Matière Condensée, CEA-Grenoble, 38054 Grenoble, France, Département de Biologie Cellulaire et Moléculaire, CEA-Saclay, 91191 Gif s/Yvette, France, Department of Chemistry, Carnegie Mellon University, Pittsburgh, Pennsylvania 15213, and Department of Chemistry and Center for Metalloenzyme Studies, University of Georgia, Athens, Georgia 30602

Received July 21, 1997; Revised Manuscript Received August 21, 1997⊗

ABSTRACT: The rubredoxin from *Clostridium pasteurianum* contains a single iron atom bound to the polypeptide chain by cysteines 6, 9, 39, and 42. The C42A variant of this protein has been prepared by site-directed mutagenesis and heterologous expression of the gene in *Escherichia coli*. The mutated protein was found to contain an unexpected chromophore that has been characterized by a variety of techniques. UV−visible absorption and resonance Raman spectra were strongly reminiscent of those of [2Fe-2S] proteins. Mössbauer spectra of the oxidized chromophore isolated in oxygen-free conditions indicated low-temperature diamagnetism resulting from antiferromagnetically coupled high-spin ferric ions. Analysis of X-ray absorption fine structure spectra yielded an Fe−Fe distance of 2.68 Å. Colorimetric assays of iron and inorganic sulfide showed that the two elements are present in a 1:1 ratio. Electrospray-ionization mass spectra displayed a major component at $M = 6190$ Da, i.e. the molecular mass of the C42A apoprotein plus two atomic masses of iron and two atomic masses of sulfur. Taken together, these data show that a mere point mutation allows the stabilization of a binuclear [2Fe-2S] cluster in a protein that normally accommodates a mononuclear Fe(Scys)$_4$ site. Assembly of a [2Fe-2S] cluster may occur because rubredoxin assumes a similar fold around its metal center as the [2Fe-2S] Rieske protein. Alternatively, a more extensive structural rearrangement of the polypeptide chain of the C42A rubredoxin variant may be considered as well.

Iron−sulfur (Fe-S) active sites display a uniquely wide range of iron nuclearities (*1*, *2*). This idiosyncrasy is a reflection of the versatile chemistry of iron−sulfide−thiolate systems, which allows the self-assembly of a variety of different structural frameworks with simple reagents (*3*, *4*). Therefore, the chemical synthesis of specific models of Fe-S active sites has often required the development of elaborate reaction conditions and strategies (*3*). In contrast, proteins exert a strong control on the assembly of their Fe-S clusters, and in any given protein site, the occurrence of only one cluster type is generally observed. Most exceptions to this rule are restricted to the [4Fe-4S] ⇔ [3Fe-4S] interconversion, which involves the reversible loss of one iron atom by a cubane cluster. In this case, however, the cubane structural framework is conserved, and therefore, no major protein rearrangement is required (*5*). Accommodation of two very different Fe-S structures by a single protein site has been observed in only very few occasions. Adrenodoxin, which normally contains a [2Fe-2S] cluster, has been reported to assemble a very unstable mononuclear FeS_4 site upon incubation of the apoprotein in the presence of iron and dithiothreitol (*6*). Conversely, rubredoxin, which in its native state contains a Fe(Scys)$_4$ site, was found to assemble an unstable [4Fe-4S] cluster upon addition of iron and sulfide to aporubredoxin in a 9:1 mixture of DMSO and H_2O (*7*). The [4Fe-4S]$^{2+}$ active site of the nitrogenase iron protein has been shown to be converted into a [2Fe-2S] cluster by oxidative degradation in the presence of iron chelators (*8*, *9*). Another [4Fe-4S] to [2Fe-2S] conversion has recently been observed upon exposure to O_2 of the FNR protein from *Escherichia coli* (*10*). Thus far, the best-characterized cluster rearrangement with a significant amplitude is the conversion of the cubane [3Fe-4S] cluster of aconitase (*11*) into a linear 3Fe cluster under alkaline conditions (*12*). However, in this case, new cysteine residues are recruited as ligands of the linear 3Fe cluster (*13*), which, according to the crystal structure of the native enzyme (*14*), implies a considerable structural reorganization of the protein, at least in the Fe-S cluster binding region (*11*).

The development of site-directed mutagenesis has allowed extensive investigation of the effects of the polypeptidic environment on the structure and properties of Fe-S active sites (reviewed in ref 15). Significant results include

† This work was supported by the National Institutes of Health (Grant GM-22701 to E.M. and Grant GM-42025 to R.A.S.). C.M.C. was partially supported by a traineeship from the NSF Research Training Group Award to the Center for Metalloenzyme Studies (DIR 90-14281).

* Author to whom correspondence should be addressed: DBMS-Métalloprotéines, CEA-Grenoble, 38054 Grenoble, France. Fax: (33) 4 76 88 58 72. E-mail: jac@ebron.ceng.cea.fr.

‡ Département de Biologie Moléculaire et Structurale, CEA-Grenoble.

§ Institut de Biologie Structurale, CEA-CNRS.

|| Département de Recherche Fondamentale sur la Matière Condensée, CEA-Grenoble.

⊥ CEA-Saclay.

@ Carnegie Mellon University.

University of Georgia.

⊗ Abstract published in *Advance ACS Abstracts,* October 1, 1997.

S0006-2960(97)01775-3 CCC: $14.00

cysteine ligand swapping (*16*, *17*), replacement of cysteine ligands by other residues (reviewed in ref 15), and deletions of protein segments in the vicinity of the Fe-S cluster (*17*). A number of interesting changes of redox potential or chromophore structure have been reported (*15*, *17*), but no modification of active site nuclearity other than the [4Fe-4S] ⇔ [3Fe-4S] interconversion (reviewed in ref 15) had yet been obtained as a result of site-directed mutagenesis. Here, we report the first such occurrence, namely the assembly of a binuclear [2Fe-2S] cluster in a molecular variant of *Clostridium pasteurianum* rubredoxin.

MATERIALS AND METHODS

All common DNA manipulations were as described (*17*−*20*). The recombinant rubredoxin from *C. pasteurianum* was purified as reported (*19*). The genes encoding the C9S and C42A[1] variants were obtained by mutagenesis of the wild type Rd gene and overexpressed in *E. coli* as described for the C42S molecular variant (*21*). The purifications of C9S and C42A *Cp*Rd were as reported (*19*, *21*). Oxygen-free conditions were used throughout.

Iron (*22*) and sulfide (*23*) were assayed by colorimetric methods.

UV−visible spectra were recorded on a Hewlett-Packard 8452 diode array spectrophotometer.

EPR spectra were recorded with a X-band Varian E-109 spectrometer equipped with a liquid helium transfer system (Oxford Instruments ESR 900) in the 8−50 K temperature range with a microwave power range of 0.01−1 mW.

Low-temperature (15−20 K) resonance Raman spectra were excited at 457.9 nm and recorded as previously described (*24*−*26*).

Amino acid analysis was performed using a Beckman model 6300 analyzer on samples hydrolyzed in the vapor of 6 N HCl containing 0.1% (w/v) phenol, for 24 h at 110 °C.

Automated Edman degradation was performed using an Applied Biosystems model 477A protein sequencer, and aminoacyl phenylthiohydantoin derivatives were identified and quantitated on-line with a model 120A HPLC system, as recommended by the manufacturer.

Electrospray-ionization mass spectra were recorded as described (*27*) on an API III+ triple-quadrupole mass spectrometer (Perkin-Elmer Sciex) equipped with a nebulizer-assisted electrospray (ion-spray) source. The instrument was tuned and calibrated in the positive mode, and polarities were inverted in the negative mode (detection of anions). The electric potential difference between the orifice (−70 V) and the adjacent electrodes was kept very low to minimize collision-induced dissociation and thus preserve the holoprotein structure. The mass spectra were averages of four scans obtained with a dwell time of 1.5 ms per 0.4 *m*/*z* step over the 700−2200 *m*/*z* range. The samples (ca. 160 μM protein in 10 mM ammonium acetate at pH 7.3) were infused into the source at a flow rate of 3 μL/min using a Harvard 22 syringe pump and a Valco CI4W1 injector equipped with a 1 μL internal loop. The pH of the infusion solvent (25% methanol and 0.1% triethylamine at pH 8.5 in H_2O) was set to minimize Fe-S cluster degradation. The reconstructed molecular mass profile was obtained by using a deconvolution algorithm (PE-Sciex).

Protein samples (in 20 mM potassium phosphate at pH 7.5) for X-ray absorption spectroscopy (XAS) were concentrated to ca. 20 mg/mL in an Amicon cell fitted with a YM3 membrane. Concentrated protein solutions (70 μL) were thoroughly mixed with glycerol (35 μL) and loaded into 20 × 4 × 1 mm^3 polycarbonate XAS cuvettes with a 0.025 mm thick Mylar window across one 20 × 4 mm^2 face. The samples were quickly frozen by plunging into liquid nitrogen and were kept in liquid nitrogen until data were collected. Iron K-edge XAS data were recorded at the Stanford Synchrotron Radiation Laboratory (SSRL) on unfocused wiggler beamline 7-3 (running at a wiggler field of 1.8 T) under dedicated ring conditions (3.0 GeV, 50−100 mA) using a Si[220] double-crystal monochromator with an upstream vertical aperture of 1 mm. Harmonic rejection was achieved by detuning one monochromator crystal to ca. 50% off peak. The incident X-ray intensity was measured with a nitrogen-filled ionization chamber, and the energy was calibrated by recording the transmission of an Fe foil (first inflection at 7111.2 eV) between a second and third ionization chamber while simultaneously recording the sample X-ray K_α fluorescence excitation spectrum using a 13-element germanium detector (*28*). The samples were maintained at a temperature of ca. 10 K during data collection, using an Oxford Instruments liquid helium flow cryostat. Eight to ten 28 min scans were collected for each sample, and the data were averaged for all valid fluorescence channels of all scans for a given sample to yield the raw XAS data. These data were processed and analyzed with the EXAFSPAK suite of programs developed by G. N. George (http://ssrl01.slac.stanford.edu/exafspak.html) using ab initio theoretical scattering phase and amplitude functions generated with the program FEFF v5.04 (*29*, *30*). No smoothing, Fourier filtering, or related manipulations were performed upon the data. The value for the threshold energy (E_0, the energy zero for k) was assumed to be 7120 eV for the Fe K-edge EXAFS.

Protein samples for Mössbauer analysis were prepared by growing *E. coli* cells containing the appropriate plasmids (*21*) in ^{57}Fe-enriched mineral medium. The latter was M9 (Life Technologies, Gaithersburg, MD) supplemented with glucose (0.2%), $MgSO_4$ (1 mM), vitamin B_1 (0.5 mg/L), and ^{57}Fe (1 mg/L). Iron metal or oxide was dissolved in a 1:1 mixture of concentrated hydrochloric and nitric acids to produce an Fe concentration of 40 mg/mL. A 100 mL culture in mineral medium was started from 0.5 mL of an overnight culture in rich medium, allowed to grow for 10 h at 30 °C, and used to inoculate (0.3% inoculum) ten 1 L cultures in mineral medium. These were grown at 30 °C for 12−14 h, until $A_{550} \geq 1$, submitted to a temperature jump for 2 h at 42 °C, and further incubated at 30 °C for 5−6 h. Cells were harvested and broken, and the protein was purified as described (*21*), except for the last anion-exchange HPLC step, which was omitted. Proteins overproduced in mineral medium were found to be satisfactorily purified after the Sephadex G-50 gel filtration. The yield of such a preparation was 10−15 mg of protein. The Mössbauer spectra were recorded with a constant acceleration spectrometer using a cryostat from Janis Research, Inc. The cryostat houses a

[1] Abbreviations: EPR, electron paramagnetic resonance; ESI-MS, electrospray-ionization mass spectrometry; EXAFS, extended X-ray absorption fine structure; Fd(s), ferredoxin(s); FT, Fourier transform; *Cp*, *C. pasteurianum*; *Cp*Rd, *C. pasteurianum* rubredoxin; PCR, polymerase chain reaction; C42A, mutated rubredoxin in which cysteine 42 has been replaced by alanine; Rd, rubredoxin; XAS, X-ray absorption spectroscopy; WT, wild type.

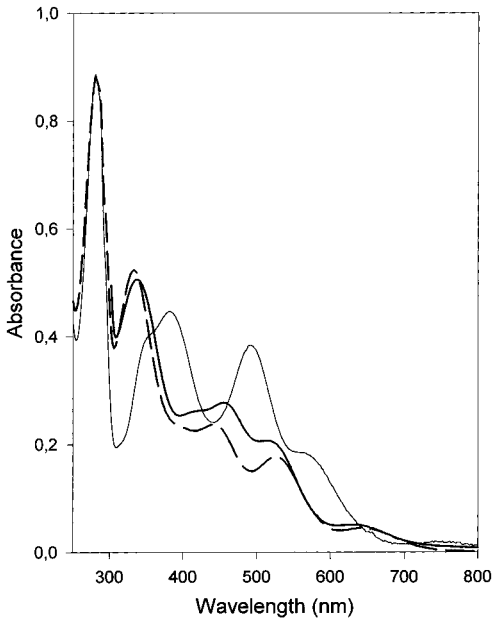

FIGURE 1: UV−visible absorption spectra of wild type (thin solid line), C9S (thick solid line), and C42S (thick dashed line) *C. pasteurianum* rubredoxins. The proteins were in 10 mM potassium phosphate (pH 8.0) and 0.5 M NaCl. The optical path length was 1 mm. The protein concentrations were 4 mg/mL for the wild type and ca. 5 mg/mL for the mutated proteins. The spectrum of the C9S protein below 300 nm was not drawn for the sake of clarity.

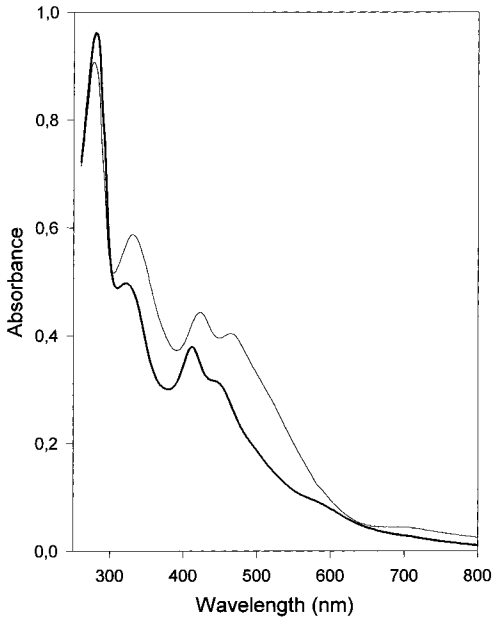

FIGURE 2: UV−visible absorption spectra of spinach ferredoxin (thin line) and of C42A *C. pasteurianum* rubredoxin (thick line). The buffer was as in Figure 1. Protein concentrations were ca. 5 mg/mL. The optical path length was 1 mm.

superconducting magnet that allows application of magnetic fields up to 8.0 T parallel to the incident γ rays.

RESULTS

In the course of our ongoing investigation of serine ligation in Fe-S clusters (reviewed in ref 15), we have prepared cysteine to serine mutated forms of *C. pasteurianum* rubredoxin (*Cp*Rd). The C42S variant has been described (*21*). The UV−visible absorption spectrum of the heretofore unreported C9S variant of *Cp*Rd is shown in Figure 1 together with those of C42S and wild type (WT) *Cp*Rd. The spectra of the two mutated forms are similar, but both differ from that of the WT protein by shifts of their absorption bands to higher energy, as expected for replacement of a sulfur ligand by oxygen (ref 21 and references therein). Whereas these data strongly suggest that the newly introduced serine residues have become ligands of the iron atom, oxygen ligation might alternatively be provided by solvent water molecules or ions. This question often arises upon cysteine to serine substitution, since proof of serine ligation by two-dimensional NMR or X-ray crystallography can only rarely be brought forth (*31*−*33*). Therefore, the role of the newly introduced serine residue as a ligand of the metal site is often assessed by substituting it with an alanine residue. The active site then is not expected to assemble if the replaced cysteine or serine residues are mandatory components of the chromophore (*15*, *20*). Following this rationale, the C42A mutated form of *Cp*Rd was prepared as a control for comparison with the C42S variant.

Extracts of *E. coli* cells transformed with the C42A mutated Rd gene and grown under conditions suitable for the overproduction of recombinant Rd were distinctly brown. Along the purification steps normally used for the purification of Rd (*19*, *21*), a brown fraction was isolated, the color of which was in strong contrast to the red color of WT Rd and of the C42S and C9S variants.

N-terminal sequencing confirmed that the brown protein was Rd. Electrospray-ionization mass spectrometry in the positive-ion detection mode, which in most cases removes the Fe-S active sites (*27*), yielded a mass of 6015 Da which matched the mass of the *C. pasteurianum* aporubredoxin (6047.5 Da, ref 34) minus the atomic mass of sulfur. These data confirm that the polypeptide chain containing the chromophore described below is the C42A variant of *Cp*Rd.

The UV−visible absorption spectrum of C42A Rd (Figure 2) differs from that of the WT protein (Figure 1) but is strongly reminiscent of those of [2Fe-2S] proteins, as shown by the comparison with the spectrum of the [2Fe-2S] spinach ferredoxin (Figure 2). The UV−visible absorption spectrum of C42A Rd differs from that of spinach Fd by shifts of its absorption bands at 322, 412, and 444 nm to higher energy (by 10−20 nm). The spectrum of C42A Rd also displays a broad band near 600 nm which is possibly a counterpart of the weak band observed in the spectra of most [2Fe-2S] ferredoxins at ca. 700 nm (see the spectrum of spinach Fd in Figure 2 and ref 20).

The 457.9 nm-excited resonance Raman (RR) spectrum of C42A Rd differs from that of the WT protein (*21*), and is in particular dominated by a strong band at 292 cm^{-1} (Figure 3). A strong band in the 280−295 cm^{-1} region is always observed in RR spectra of $[2Fe\text{-}2S]^{2+}$ clusters excited at 457.9 nm (*35*−*38*; see Table 1) but not in those of [1Fe] (*21*), [3Fe-4S] (*39*), or [4Fe-4S] clusters (*26*). Furthermore, the pattern consisting of four main bands (292, 330, 363, and 398 cm^{-1}) in the 250−400 cm^{-1} range (Figure 3), where the Fe-S stretching modes are expected to occur, is altogether very similar to those previously reported for several [2Fe-2S] proteins (*20*, *35*−*38*).

The only EPR feature displayed by as-isolated C42A Rd was a very weak EPR signal in the $g = 4.3$ region in the 4−40 K temperature range (spectrum not shown). The signal, normalized to the concentration of the protein, was 50-fold weaker than the signals of WT or C42S Rd (*21*). Thus, the C42A Rd as isolated is essentially EPR silent. Upon addition of dithionite, the chromophore was bleached ir-

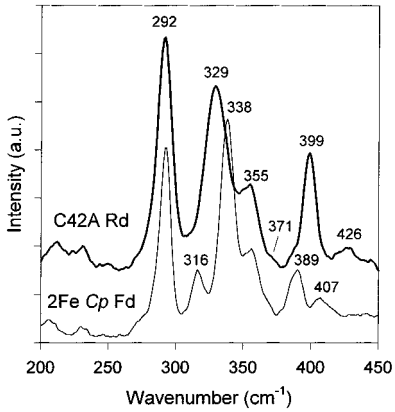

FIGURE 3: Resonance Raman spectra, excited at 457.9 nm, of the C42A variant of *C. pasteurianum* rubredoxin (thick line) and of wild type [2Fe-2S] *C. pasteurianum* Fd (thin line). The temperature was 20−25 K. The scanning speed was 50 cm^{-1}/min. The time constant was 1.8 s. Both spectra were obtained by the summation of six scans.

Table 1: Resonance Raman Frequencies (cm^{-1}) of Several [2Fe-2S] Ferredoxins and of C42A *C. pasteurianum* Rd[a]

assignments[b]	2Fe*Cp*Fd[c] (WT)	spinach Fd[c]	adrenodoxin[d]	C42A Rd
B_{3u}^T	292	285	291	292
B_{1g}^B	316	330	317	nd[e]
A_g^T	338	340	329	329
B_{1u}^T, B_{2g}^T	356	355	341	355
B_{3u}^B	370	369	349	371 (wsh[f])
A_g^B	390	397	393	399
B_{2u}^B	407	428	421	426

[a] Spectra excited at 457.9 nm. [b] Assignments of the Fe-S stretching modes in the idealized D_{2h} point group of the $Fe_2S_2^BS_4^T$ chromophore (*36*, *37*). B = bridging (inorganic sulfur), and T = terminal (cysteinyl sulfur). [c] Reference 35. [d] Reference 36. [e] nd, not detected. [f] wsh, weak shoulder.

reversibly in a few tens of seconds. Rapid (within 5−10 s) freezing of samples upon reduction allowed the detection of a nearly axial signal with $g = 2.04$, 1.93, and 1.94 (Figure 4). The intensity of this signal was 5−7% of that expected if all the iron present was involved in a $[2Fe\text{-}2S]^+$ cluster. The signal was still observed, though broadened, at 50 K, a temperature where signals arising from $[4Fe\text{-}4S]^+$ clusters would usually not be detected. The power saturation properties of the C42A Rd EPR signal at 10 K (not shown) demonstrate that it relaxes faster than plant type or *C. pasteurianum* [2Fe-2S] Fds.

Mössbauer spectra of as-isolated C42A Rd have been recorded at 4.2 K in applied fields of 0.05 T (Figure 5A) and 8.0 T (Figure 5B). The spectrum of Figure 5A shows a quadrupole doublet with an average isomer shift, $\delta = 0.32$ mm/s, and quadrupole splitting, $\Delta E_Q = 0.55$ mm/s. The simulation of the 8.0 T spectrum in Figure 5B was performed by assuming that the electronic ground state of the chromophore is diamagnetic. The good quality of the fit confirms this assumption. The only Fe-S clusters which have an $S = 0$ ground state are $[2Fe\text{-}2S]^{2+}$ and $[4Fe\text{-}4S]^{2+}$. In the former, the two iron sites are in the 3+ oxidation state which typically exhibits δ values of 0.28 mm/s, while in the latter, the four iron sites are (formally) in a 2.5+ oxidation state and have δ values of 0.45 mm/s. Therefore, the observed diamagnetism together with the values for δ and ΔE_Q unequivocally identifies the chromophore in C42A Rd as a binuclear cluster involving two coupled ferric ions. Data

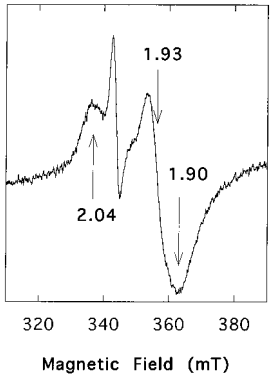

FIGURE 4: EPR spectrum of reduced C42A *C. pasteurianum* rubredoxin recorded at 10 K. The microwave frequency was 9.648 GHz, the microwave power 0.1 mW, the modulation frequency 100 kHz, and the modulation amplitude 1 mT.

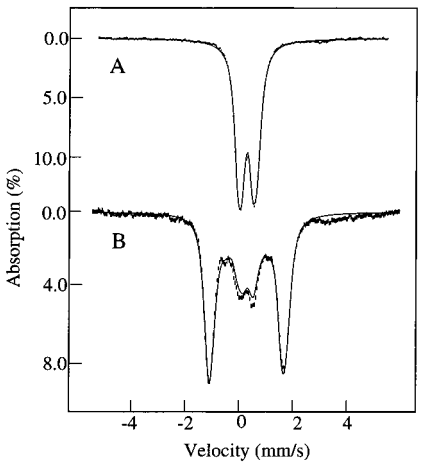

FIGURE 5: Mössbauer spectra of C42A *C. pasteurianum* rubredoxin recorded at 4.2 K in parallel applied fields of 0.05 T (A) and 8.0 T (B). Solid lines are spectral simulations assuming a diamagnetic center containing two sites with a $\Delta E_Q(1)$ of 0.72 mm/s and a $\delta(1)$ of 0.30 mm/s and a $\Delta E_Q(2)$ of 0.40 mm/s and a $\delta(2)$ of 0.29 mm/s. For the simulation of the 8.0 T spectra, the asymmetry parameter $\eta = 1$ for both sites. The shallow absorption between the +3 and +4 mm/s Doppler velocity in the 8.0 T spectrum is due to the presence of approximately 7% high-spin ferrous contaminant. Its contribution to the 0.5 T spectrum has been removed.

shown below further demonstrate that this cluster is of the $[2Fe\text{-}2S]^{2+}$ type.

The Mössbauer absorption lines of $[2Fe\text{-}2S]^{2+}$ clusters in general are quite narrow and have Lorentzian shapes. A careful analysis of the spectrum of Figure 5A indicates that it cannot be described by one quadrupole doublet with Lorentzian lines, but that it can be fitted satisfactorily by a sum of two doublets comprising four lines at Doppler velocities of −0.08, 0.10, 0.48, and 0.67 mm/s. These lines can be assigned either to two nested doublets (case 1) with $\Delta E_Q(1) = 0.72$ mm/s and $\delta(1) = 0.30$ mm/s and $\Delta E_Q(2) = 0.40$ mm/s and $\delta(2) = 0.29$ mm/s or to two overlapping doublets (case 2) with $\Delta E_Q(1) = 0.58$ mm/s and $\delta(1) = 0.22$ mm/s and $\Delta E_Q(2) = 0.58$ mm/s and $\delta(2) = 0.38$ mm/s. The observation of two, albeit unresolved, doublets is not unexpected since there are only three cysteine residues per monomer available for cluster coordination; in a Fe_2S_2-$(Cys)_3X$ cluster, the iron sites cannot be identical. However, the isomer shift for Fe^{3+} sites in $[2Fe\text{-}2S]^{2+}$ clusters is only moderately sensitive to the ligand environment. For instance, the complexes $[Fe_2S_2(PhS)_4]^{2+}$, $[Fe_2S_2(C_4H_4N)_4]^{2+}$, and $[Fe_2S_2(PhO)_4]^{2+}$ have δ values of 0.28, 0.26, and 0.38 mm/s, respectively (ref 40 and references therein). Moreover,

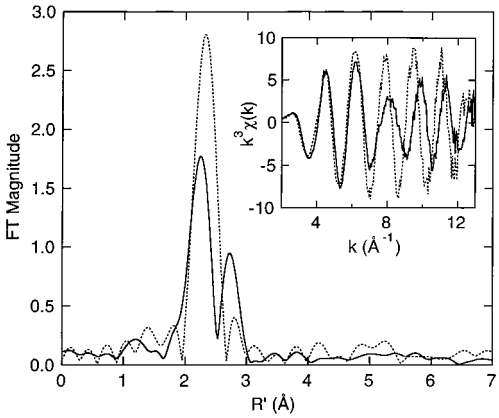

FIGURE 6: Fourier transforms of Fe EXAFS of wild type (dashed line) and C42A (solid line) *C. pasteurianum* rubredoxin. The inset compares the Fe EXAFS data for the same derivatives. The Fourier transforms were performed over the k range of 2−13 Å^{-1} with k^3 weighting and were phase-corrected for Fe-S scattering.

in [2Fe-2S]$^{2+}$ (*41*) and [1Fe] (C. Achim, S.-J. Yoo, J. Meyer, and E. Münck, unpublished) active sites, the replacement of one cysteine ligand by a serine resulted in only marginal variations of δ. For these reasons, the nested assignment of case 1 is more likely.

The Fourier transforms of the Fe K-edge EXAFS of C42A Rd differ significantly from those of the WT protein, displaying two major peaks which can be assigned to Fe-S scattering (at $R' = 2.3$ Å in the phase-corrected FT) and to Fe-Fe scattering (at $R' = 2.8$ Å) (Figure 6). This FT is very reminiscent of the Fe EXAFS FT normally observed for [2Fe-2S] ferredoxins (*42*). Curve fitting results (summarized in Table 2 and Figure 7) are consistent with an average FeS_4-Fe_1 coordination environment with Fe-S and Fe-Fe distances of 2.22 and 2.68 Å, respectively. Splitting the Fe-S shell into two (as would be expected for different Fe-S_{bridge} vs Fe-$S_{terminal}$ bond lengths) results in insignificant improvement in the fit (cf. fits 2 and 3 in Table 2).

Colorimetric assays of iron and inorganic sulfide showed that the Fe:S^{2-} ratio in C42A Rd is 1.0 ± 0.07 (mean of eight determinations) and thus consistent with the presence of a [2Fe-2S] cluster. Correlation of iron analyses with UV−visible absorption yielded a molar extinction coefficient at 412 nm of 10 200 ± 500 M^{-1} cm^{-1} for the [2Fe-2S] cluster.

The stoichiometry of the [2Fe-2S] cluster with respect to the polypeptide chain was determined by correlating iron and amino acid analyses. For a sample with an A_{412}/A_{280} of 0.32, the measurements yielded 0.77 ± 0.1 iron atom per C42A Rd polypeptide chain. For the sample of which the UV−visible spectrum is shown in Figure 2 (A_{412}/A_{280} = 0.38), the measured ratio was 1.2 ± 0.15 iron atoms per

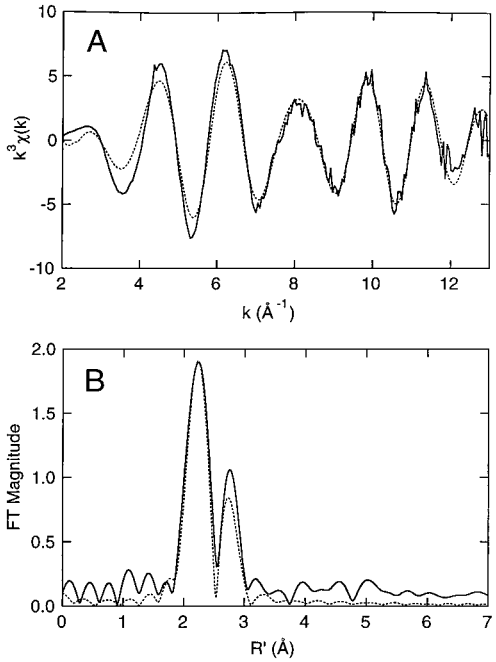

FIGURE 7: Curve-fitting simulation (dashed line) compared to the observed (solid line) Fe EXAFS (A) and FT (B) of C42A *C. pasteurianum* rubredoxin. The simulation represents fit 2 in Table 2.

polypeptide chain. Considering that the measured iron stoichiometries are most often lower than those expected, in particular for the less stable proteins, the values reported above would indicate the presence of one [2Fe-2S] cluster per polypeptide chain.

The chemical composition of the active site of C42A Rd has been confirmed by electrospray-ionization mass spectrometry (ESI-MS). In the positive-ion detection mode, the Fe-S active sites are often disrupted, and then, only the contribution of the apoprotein is observed in the spectra (*27*). In contrast, the negative-ion detection mode, which can be implemented at neutral pH with the acidic rubredoxins and ferredoxins, allows the determination of molecular masses of holoproteins, and the chemical composition of the inorganic Fe-S cores can thereby be obtained (*27*, *43*). An ESI-MS spectrum of C42A Rd recorded under such conditions is shown in Figure 8. A peak arising from the apoprotein is observed at $M = 6013.7$ Da, but the major peak at $M = 6189.2$ Da corresponds to the mass of the apoprotein plus two iron and two sulfur atoms. A few peaks arising from Na^+ and K^+ adducts, as well as from cluster degradation intermediates, were also observed. The nondeconvoluted spectra (not shown) displayed no detectable contribution from oligomeric forms of the protein.

Table 2: Curve Fitting Results for Fe EXAFS of C42A *C. pasteurianum* Rd[a]

sample	data range	fit (data)	shell	N_s	R_{as} (Å)	σ_{as}^2 (Å^2)	ΔE_0 (eV)	f'[b]
C42A *Cp* Rd	k = 2.0−13.0 Å^{-1}	1 (raw)	Fe-S	(4)[c]	2.22	0.0058	1.95	0.099
		2	Fe-Fe	(1)	2.68	0.0032	2.09	0.063
		(raw)	Fe-S	(4)	2.22	0.0061	[2.09][c]	<0.050>[e]
		3	Fe-Fe	(1)	2.67	0.0026	2.28	0.061
		(raw)	Fe-S	(2)	2.29	0.0018	[2.28]	<0.048>
			Fe-S	(2)	2.18	0.0023	[2.28]	

[a] N_s is the number of scatterers (or groups) per metal. R_{as} is the metal−scatterer distance. σ_{as}^2 is a mean square deviation in R_{as}. ΔE_0 is the shift in E_0 for the theoretical scattering functions. [b] f' is a normalized error (χ^2): $f' = \{\sum_i[k^3(\chi_i^{obs} - \chi_i^{calc})]^2/N\}^{1/2}/[(k^3\chi^{obs})_{max} - (k^3\chi^{obs})_{min}]$. [c] Numbers in parentheses were not varied during optimization. [d] Numbers in square brackets were constrained to be a multiple of the above value. [e] Numbers in angle brackets are f' for the smoothed data.

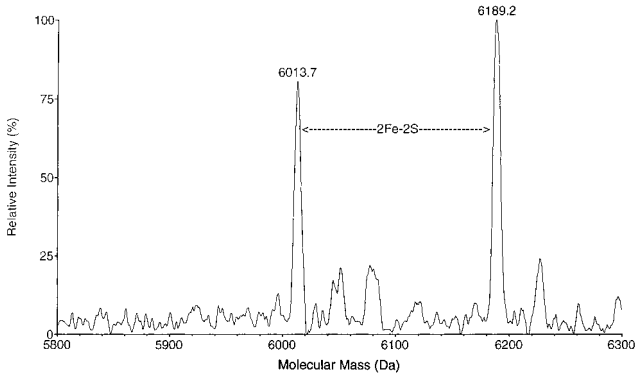

FIGURE 8: Reconstructed electrospray-ionization mass spectrum, in the negative-ion detection mode, of C42A *C. pasteurianum* rubredoxin. The deconvolution was performed on the five- to eight-charge peaks in the 700−1600 *m*/*z* window of the experimental spectrum (not shown). The main features correspond to the apoprotein (6013.7 ± 1 Da) and to the holoprotein containing one [2Fe-2S] cluster (6189.2 ± 1 Da). Most minor components arise from sodium or potassium adducts and from cluster degradation intermediates (in the 6060−6120 Da range for the latter).

In solution, according to gel filtration runs on Sephadex G-50, the C42A Rd variant assumed an oligomeric structure, in contrast to the monomeric WT Rd. Dimeric and tetrameric forms appeared to be present, with little dependence on the ionic strength of the solvent (0.05−2 M NaCl). When the fractions isolated by gel filtration were rerun on the same column, a significant extent of interconversion of the oligomeric forms was observed, possibly resulting from a dynamic equilibrium. The UV−visible absorption spectra of the various oligomers separated by gel filtration were identical, suggesting that the inter-polypeptide interactions do not involve the chromophore.

DISCUSSION

The combined spectroscopic (UV−visible absorption, resonance Raman, EPR, Mössbauer, and EXAFS) and analytical (mass spectrometry, iron and sulfide assays, and amino acid analysis) data gathered here demonstrate compellingly that the C42A variant of *Cp*Rd contains a [2Fe-2S] cluster. However, the means by which this cluster is stabilized by the polypeptide chain remain to be fully elucidated. Given the significantly different geometries of the mononuclear and binuclear Fe-S sites, it is difficult to predict the details of the rearrangement of the polypeptide chain implied by such a change. For comparison, we refer to the incorporation of a binuclear copper site into the blue copper protein azurin (*44*), which required the insertion of three residues and the deletion of one residue in the ligand loop. Surprisingly, an analogous change in nuclearity has occurred in the C42A Rd variant upon a mere point mutation.

The structural rearrangements of the polypeptide chain associated with the incorporation of a [2Fe-2S] cluster in C42A Rd might be significant, in view of the apparent changes in quaternary structure resulting from this mutation. However, a conservative interpretation requiring only limited alterations of the polypeptide structure may be derived from the crystal structure of a Rieske protein fragment (*45*). Rather unexpectedly, the polypeptide fold around the [2Fe-2S] cluster of the latter protein was found to be quite similar to that observed around the single Fe atom in Rd (*46*). Indeed, the two cysteinyl sulfur ligands, the Fe atom to which they are bound, and the two inorganic sulfur atoms of the Rieske protein can be nearly superimposed with the Cys6 and Cys39 cysteinyl sulfur atoms, the iron atom, and the Cys9 and Cys42 sulfur atoms, respectively, of Rd (*45*). The "outer" half of the Rieske active site, which is absent from Rd, consists of a second iron atom and of two histidine ligands. The Cα atoms of the latter two residues occur in spatial positions corresponding to those of Cys42 and Val8 of *Cp*Rd, but their side chains are significantly tilted outward from the molecule (*45*). In view of the similarities between the two proteins, the assembly of a [2Fe-2S] cluster in C42A Rd might be rationalized as follows. The removal of the Cys42 sulfur atom, combined with a displacement of Cys9, could open the Rd active site cavity and allow the additional incorporation of two inorganic sulfurs and of a second iron atom. Both a rotation of the side chain of Cys9 and a shift of the Cα chain (by ca. 1 Å) would be required to make room for a [2Fe-2S] cluster, and would then possibly allow Cys9 to become a ligand of the outer iron atom. Whereas ligation by Cys9 is by no means demonstrated, it is deemed likely, because it would provide the [2Fe-2S] cluster with a third anchoring point on the polypeptide chain, consistent with its relative stability, as assessed, for instance, by the ESI-MS data (Figure 8).

The coordination of the [2Fe-2S] cluster in C42A Rd requires a fourth ligand which could be furnished either by the same polypeptide chain or by an external donor, which may be either another C42A Rd molecule or a solvent molecule. Since any such adduct is likely to be removed under the conditions of the electrospray, the ESI-MS data are not expected to be of use for the identification of the fourth ligand. The observation of oligomeric forms of the protein in gel filtration experiments might suggest the involvement of more than one C42A Rd polypeptide chain in the ligation of one cluster. Then, however, the ratio of iron to protein should not exceed 1 (1 [2Fe-2S] cluster per protein dimer), and would most probably be significantly lower, whereas a value of 1.2 ± 0.15 has been experimentally determined.

Some spectroscopic features of the [2Fe-2S] chromophore of C42A Rd are suggestive of noncysteinyl, possibly oxygen, ligation. For instance, the UV−visible absorption bands of C42A Rd in the 300−600 nm region differ from those of benchmark [2Fe-2S] Fd by hypsochromic shifts of 10 nm near 300 nm, 20 nm near 400 nm, and up to 80 nm for the low-energy band near 700 nm (Figure 2). Similar band shifts have previously been reported upon replacement of cysteine ligands by serine in the [2Fe-2S] *C. pasteurianum* Fd and are consistent with partial replacement of sulfur by oxygen ligation (*20*). The Mössbauer data suggest the presence of two distinct ferric sites and would thus be consistent with noncysteinyl ligation on one of the iron atoms. However, they provide no information regarding the nature of the heteroligand. The replacement of a cysteine ligand by serine in the C56S and C60S variants of [2Fe-2S] *C. pasteurianum* Fd has been shown to result in 4−10 cm^{-1} upshifts of the two RR bands near 290 and 330−350 cm^{-1} (*20*) which, despite significant kinematic coupling between bridging and terminal modes (*35*), have been shown to arise mainly from Fe-Scys stretching modes (*36, 37*). The relevant bands at 292 and 329 cm^{-1} in the 457.9 nm-excited spectrum of C42A Rd (Figure 3) do not occur outside the range observed for all-cysteine ligated clusters (*20, 38*). However, many other factors contribute to the frequencies of these modes (*37*), and oxygen ligation should not be expected to systematically result in upshifts of RR bands. Indeed, in some variants of the [2Fe-2S] *C. pasteurianum* Fd most likely involving

oxygen ligation, e.g. C14A/C24A, downshifts of some bands attributed to Fe-Scys stretching modes were even observed (*20*). Information on the fourth ligand of the C42A Rd cluster might also be expected from the EXAFS data. For instance, spectra of the C42S Rd variant, in which one of the four cysteine ligands of the iron has been replaced by serine (*21*), were found to differ significantly from those of the WT protein (C. M. Colangelo, R. A. Scott, and J. Meyer, unpublished). In contrast, single cysteine to serine mutations in a [2Fe-2S] Fd result in a ratio of oxygen to sulfur ligation of only 0.5:3.5, vs 1:3 in Rd. Accordingly, the changes in the EXAFS spectra are insignificant (C. M. Colangelo, R. A. Scott, and J. Meyer, unpublished). Therefore, the presence of a noncysteinyl ligand in C42A Rd would probably not be detectable in EXAFS spectra, especially since no reference EXAFS spectrum of the same chromophore with all-cysteine ligation is available.

A [2Fe-2S] cluster is undoubtedly present in the C42A Rd variant. The unprecedented incorporation of a binuclear cluster in a polypeptide chain that normally accommodates a single iron atom may to a certain extent be rationalized on the basis of similarities between the polypeptide folds of Rd and of the Rieske protein. This finding opens up new perspectives on how proteins can use the intrinsic versatility of iron−sulfur clusters in order to fulfill their biological functions (*4*). The possibility of accommodating Fe-S active sites of different nuclearities in thermodynamically stable conformations of a single protein is demonstrated here for the [1Fe]/[2Fe-2S] couple. New means of iron uptake or release with associated conformational changes are thus suggested. Other features of this system, in particular the set of ligands involved, the stability, and the redox properties, are being further investigated by site-directed mutagenesis and spectroscopy.

ACKNOWLEDGMENT

Thanks are due to J.-P. Issartel for the synthesis of oligonucleotides, to J.-P. Andrieu for protein sequence analysis, and to J.-M. Moulis for discussions and comments.

REFERENCES

1. Johnson, M. K. (1994) in *Encyclopedia of Inorganic Chemistry* (King, R. B., Ed.) Vol. 4, pp 1896−1915, Wiley, Chichester, U.K.
2. Holm, R. H., Kennepohl, P., and Solomon, E. I. (1996) *Chem. Rev. 96*, 2239−2314.
3. Hagen, K. S., Watson, A. D., and Holm, R. H. (1983) *J. Am. Chem. Soc. 105*, 3905−3913.
4. Beinert, H., Holm, R. H., and Münck, E. (1997) *Science 277*, 653−659.
5. Holm, R. H. (1992) *Adv. Inorg.Chem. 38*, 1−71.
6. Sugiura, Y., Ishizu, K., and Kimura, T. (1974) *Biochem. Biophys. Res. Commun. 60*, 334−340.
7. Christou, G., Ridge, B., and Rydon, H. N. (1979) *J. Chem. Soc., Chem. Commun.*, 20−21.
8. Anderson, G. L., and Howard, J. B. (1984) *Biochemistry 23*, 2118−2122.
9. Ryle, M. J., Lanzilotta, W. N., Seefeldt, L. C., Scarrow, R. C., and Jensen, G. M. (1996) *J. Biol. Chem. 271*, 1551−1557.
10. Khoroshilova, N., Popescu, C., Münck, E., Beinert, H., and Kiley, P. J. (1997) *Proc. Natl. Acad. Sci. U.S.A. 94*, 6087−6092.
11. Beinert, H., Kennedy, M. C., and Stout, C. D. (1996) *Chem. Rev. 96*, 2335−2373.
12. Kennedy, M. C., Kent, T. A., Emptage, M., Merkle, H., Beinert, H., and Münck, E. (1984) *J. Biol. Chem. 259*, 14463−14471.
13. Plank, D. W., Kennedy, M. C., Beinert, H., and Howard, J. B. (1989) *J. Biol. Chem. 264*, 20385−20393.
14. Robbins, A. H., and Stout, C. D. (1989) *Proteins: Struct., Funct., Genet. 5*, 289−312.
15. Moulis, J.-M., Davasse, V., Golinelli, M.-P., Meyer, J., and Quinkal, I. (1996) *J. Biol. Inorg. Chem. 1*, 2−14.
16. Martín, A. E., Burgess, B. K., Stout, C. D., Cash, V. L., Dean, D. R., Jensen, G. M., and Stephens, P. J. (1990) *Proc. Natl. Acad. Sci. U.S.A. 87*, 598−602.
17. Golinelli, M.-P., Akin, L. A., Crouse, B. R., Johnson, M. K., and Meyer, J. (1996) *Biochemistry 35*, 8995−9002.
18. Ausubel, F. M., Brent, R., Kingston, R. E., Moore, D. D., Seidman, J. G., Smith, J. A., and Struhl, K. (1988) *Current Protocols in Molecular Biology*, Wiley-Interscience, New York.
19. Mathieu, I., Meyer, J., and Moulis, J.-M. (1992) *Biochem. J. 285*, 255−262.
20. Meyer, J., Fujinaga, J., Gaillard, J., and Lutz, M. (1994) *Biochemistry 33*, 13642−13650.
21. Meyer, J., Gaillard, J., and Lutz, M. (1995) *Biochem. Biophys. Res. Commun. 212*, 827−833.
22. Meyer, J., Bruschi, M. H., Bonicel, J. J., and Bovier-Lapierre, G. E. (1986) *Biochemistry 25*, 6054−6061.
23. Brumby, P. E., Miller, R. W., and Massey, V. (1965) *J. Biol. Chem. 240*, 2222−2228.
24. Lutz, M. (1977) *Biochim. Biophys. Acta 460*, 408−430.
25. Lutz, M., Moulis, J.-M., and Meyer, J. (1983) *FEBS Lett. 163*, 212−216.
26. Moulis, J.-M., Meyer, J., and Lutz, M. (1984) *Biochemistry 23*, 6605−6613.
27. Pétillot, Y., Forest, E., Meyer, J., and Moulis, J.-M. (1995) *Anal. Biochem. 228*, 56−63.
28. Cramer, S. P., Tench, O., Yocum, M., and George, G. N. (1988) *Nucl. Instrum. Methods Phys. Res., Sect. A 266*, 586−591.
29. Rehr, J. J., Mustre de Leon, J., Zabinsky, S. I., and Albers, R. C. (1991) *J. Am. Chem. Soc. 113*, 5135−5140.
30. Mustre de Leon, J., Rehr, J. J., Zabinsky, S. I., and Albers, R. C. (1990) *Phys. Rev. B 44*, 4146−4156.
31. Cheng, H., Xia, B., Reed, G. H., and Markley, J. L. (1994) *Biochemistry 33*, 3155−3164.
32. Calzolai, L., Gorst, C. M., Zhao, Z.-H., Teng, Q., Adams, M. W. W., and La Mar, G. N. (1995) *Biochemistry 34*, 11373−11384.
33. Bentrop, D., Bertini, I., Capozzi, F., Dikiy, A., Eltis, L., and Luchinat, C. (1996) *Biochemistry 35*, 5928−5936.
34. Pétillot, Y., Forest, E., Mathieu, I., Meyer, J., and Moulis, J.-M. (1993) *Biochem. J. 296*, 657−661.
35. Meyer, J., Moulis, J.-M., and Lutz, M. (1986) *Biochim. Biophys. Acta 873*, 108−118.
36. Han, S., Czernuszewicz, R. S., Kimura, T., Adams, M. W. W., and Spiro, T. G. (1989) *J. Am. Chem. Soc. 111*, 3505−3511.
37. Fu, W., Drozdzewski, P. M., Davies, M. D., Sligar, S. G., and Johnson, M. K. (1992) *J. Biol. Chem. 267*, 15502−15510.
38. Crouse, B. R., Sellers, V. M., Finnegan, M. G., Dailey, H. A., and Johnson, M. K. (1996) *Biochemistry 35*, 16222−16229.
39. Johnson, M. K., Czernuszewicz, R. S., Spiro, T. G., Fee, J. A., and Sweeney, W. V. (1983) *J. Am. Chem. Soc. 105*, 6671−6678.
40. Salifoglou, A., Simopoulos, A., Kostikas, A., Dunham, R. W., Kanatzidis, M. G., and Coucouvanis, D. (1988) *Inorg. Chem. 27*, 3394−3406.
41. Achim, C., Golinelli, M.-P., Bominaar, E. L., Meyer, J., and Münck, E. (1996) *J. Am. Chem. Soc. 118*, 8168−8169.
42. Teo, B.-K., Shulman, R. G., Brown, G. S., and Meixner, A. E. (1979) *J. Am. Chem. Soc. 101*, 5624−5631.
43. Pétillot, Y., Golinelli, M.-P., Forest, E., and Meyer, J. (1995) *Biochem. Biophys. Res. Commun. 210*, 686−694.
44. Hay, M., Richards, J. H., and Lu, Y. (1996) *Proc. Natl. Acad. Sci. U.S.A. 93*, 461−464.
45. Iwata, S., Saynovits, M., Link, T. A., and Michel, H. (1996) *Structure 4*, 567−579.
46. Dauter, Z., Wilson, K. S., Sieker, L. C., Moulis, J.-M., and Meyer, J. (1996) *Proc. Natl. Acad. Sci. U.S.A. 93*, 8836−8840.

BI971775W